

<https://helda.helsinki.fi>

Identification of factors required for m6A mRNA methylation in Arabidopsis reveals a role for the conserved E3 ubiquitin ligase HAKAI

Ruzicka, Kamil

2017-07

Ruzicka , K , Zhang , M , Campilho , A , Bodi , Z , Kashif , M , Saleh , M , Eeckhout , D , El Showk , S N , Li , H , Zhong , S , Jaeger , G D , Mongan , N P , Hejatko , J , Helariutta , Y E & Fray , R G 2017 , ' Identification of factors required for m6A mRNA methylation in Arabidopsis reveals a role for the conserved E3 ubiquitin ligase HAKAI ' , New Phytologist , vol. 215 , no. 1 , pp. 157-172 . <https://doi.org/10.1111/nph.14586>

<http://hdl.handle.net/10138/224304>

<https://doi.org/10.1111/nph.14586>

cc_by

publishedVersion

Downloaded from Helda, University of Helsinki institutional repository.

This is an electronic reprint of the original article.

This reprint may differ from the original in pagination and typographic detail.

Please cite the original version.

Identification of factors required for m⁶A mRNA methylation in *Arabidopsis* reveals a role for the conserved E3 ubiquitin ligase HAKAI

Kamil Růžicka^{1,2}, Mi Zhang³, Ana Campilho^{2,4*}, Zsuzsanna Bodi^{3*}, Muhammad Kashif², Mária Saleh¹, Dominique Eeckhout^{5,6}, Sedeer El-Showk², Hongying Li^{3,7}, Silin Zhong^{3,8}, Geert De Jaeger^{5,6}, Nigel P. Mongan⁹, Jan Hejácíko¹, Ykä Helariutta^{2,10} and Rupert G. Fray³

¹Functional Genomics and Proteomics of Plants, Central European Institute of Technology and National Centre for Biomolecular Research, Masaryk University, 62500 Brno, Czech Republic;

²Institute of Biotechnology, University of Helsinki, 00014 Helsinki, Finland; ³Plant Sciences Division, School of Biosciences, University of Nottingham, Sutton Bonington Campus,

Loughborough, LE12 5RD, UK; ⁴Research Center in Biodiversity and Genetic Resources, University of Porto, 4485-661 Vairão, Portugal; ⁵Department of Plant Systems Biology, VIB, 9052

Gent, Belgium; ⁶Department of Plant Biotechnology and Bioinformatics, Ghent University, 9052 Gent, Belgium; ⁷Key Laboratory of Crop Gene Resources and Germplasm Enhancement on

Loess Plateau, Ministry of Agriculture, Taiyuan, Shanxi 030031, China; ⁸The State Key Laboratory of Agrobiotechnology, The School of Life Sciences, The Chinese University of Hong Kong,

Hong Kong, China; ⁹School of Veterinary Medicine and Sciences, University of Nottingham, Sutton Bonington Loughborough, LE12 5RD, UK; ¹⁰Sainsbury Laboratory, University of

Cambridge, Cambridge, CB2 1LR, UK

Summary

- N⁶-adenosine methylation (m⁶A) of mRNA is an essential process in most eukaryotes, but its role and the status of factors accompanying this modification are still poorly understood.
- Using combined methods of genetics, proteomics and RNA biochemistry, we identified a core set of mRNA m⁶A writer proteins in *Arabidopsis thaliana*.
- The components required for m⁶A in *Arabidopsis* included MTA, MTB, FIP37, VIRILIZER and the E3 ubiquitin ligase HAKAI. Downregulation of these proteins led to reduced relative m⁶A levels and shared pleiotropic phenotypes, which included aberrant vascular formation in the root, indicating that correct m⁶A methylation plays a role in developmental decisions during pattern formation.
- The conservation of these proteins amongst eukaryotes and the demonstration of a role in writing m⁶A for the E3 ubiquitin ligase HAKAI is likely to be of considerable relevance beyond the plant sciences.

Authors for correspondence:

Kamil Růžicka

Tel: +420 5 4949 7904

Email: kamil.ruzicka@ceitec.muni.cz

Ykä Helariutta

Tel: +44 1223 761144

Email: yrjo.helariutta@slcu.cam.ac.uk

Rupert Fray

Tel: +44 115 951 6371

Email: rupert.fray@nottingham.ac.uk

Received: 27 January 2017

Accepted: 19 March 2017

New Phytologist (2017) 215: 157–172

doi: 10.1111/nph.14586

Key words: *Arabidopsis*, HAKAI, mRNA methylation, N⁶-adenosine methylation (m⁶A), protoxylem, VIRILIZER.

Introduction

More than 150 nucleotide modifications of RNA have been described and of these >10 have been reported in mRNA (Machnicka *et al.*, 2013). N⁶-methyladenosine (m⁶A) is the most prevalent internal mRNA modification found in eukaryotes, and has received a burst of interest in recent years (Meyer & Jaffrey, 2014; Fray & Simpson, 2015; Yue *et al.*, 2015). m⁶A appears to be involved in a broad range of biological processes including mRNA

export from the nucleus (Fustin *et al.*, 2013), regulation of splicing (Alarcón *et al.*, 2015b; Haussmann *et al.*, 2016; Lence *et al.*, 2016), mRNA translatability and stability (Wang *et al.*, 2014a,b, 2015; Bodi *et al.*, 2015; Zhou *et al.*, 2015), alternative polyadenylation site choice (Ke *et al.*, 2015) and other mechanisms accompanying RNA maturation (Meyer & Jaffrey, 2014; Yue *et al.*, 2015). m⁶A is essential for the earliest stages of pattern formation in plants (Zhong *et al.*, 2008; Bodi *et al.*, 2012; Shen *et al.*, 2016) and metazoans (Meyer & Jaffrey, 2014; Geula *et al.*, 2015; Yue *et al.*, 2015; Haussmann *et al.*, 2016; Lence *et al.*, 2016), linked with diseases in humans and other mammalian species (Jia *et al.*, 2011; Zheng *et al.*,

*These authors contributed equally to this work.

2013) and is required for meiosis in *Saccharomyces cerevisiae* (Clancy *et al.*, 2002). Reduced levels of m⁶A also affect circadian period (Fustin *et al.*, 2013) and are critical for stem cell differentiation in mammals (Geula *et al.*, 2015).

Although m⁶A can be present throughout the primary transcript, it is enriched at 3' ends, particularly within the last exon of mature mRNA (Bodi *et al.*, 2012; Dominissini *et al.*, 2012; Li *et al.*, 2014; Luo *et al.*, 2014; Ke *et al.*, 2015; Wan *et al.*, 2015). m⁶A is found within a conserved consensus sequence (G/A)(G/A) ACU (with a preference for (G/A)GACU) in different eukaryotes (Horowitz *et al.*, 1984; Narayan & Rottman, 1988; Dominissini *et al.*, 2012; Meyer *et al.*, 2012; Luo *et al.*, 2014; Wan *et al.*, 2015). However, only a subset of potential sites is actually modified and the mechanisms underlying the specificity of writing are not yet understood.

The S-adenosyl methionine dependent methyltransferase METTL3 was first purified and characterized by Bokar *et al.* (1997), as a 70-kDa subunit of a larger protein complex. Whilst METTL3 was part of a 200-kDa complex, a further 875-kDa complex component(s) was required for its *in vitro* activity (Bokar *et al.*, 1994, 1997). The identity of any of the other proteins that act together with METTL3 remained unknown until it was shown in *Arabidopsis* that FIP37 (FKBP12 INTERACTING PROTEIN 37) was a partner protein of MTA (the homologue of METTL3) (Zhong *et al.*, 2008; Shen *et al.*, 2016). Following this initial discovery, the homologues of FIP37, *S. cerevisiae* MUM2 (Muddled Meiosis 2), and mammalian WTAP (Wilms tumour 1 associated protein), were shown to interact with METTL3 (MTA) orthologues and to be required for mRNA methylation in their respective model organisms (Agarwala *et al.*, 2012; Ping *et al.*, 2014; Wang *et al.*, 2014b; Liu *et al.*, 2015). More recently, another human methylase, METTL14, phylogenetically related to METTL3 (Bujnicki *et al.*, 2002), was shown to form a complex with METTL3 and WTAP, and to be required also for m⁶A formation (Ping *et al.*, 2014; Wang *et al.*, 2014b; Liu *et al.*, 2015).

Other factors in addition to METTL3, METTL14 and WTAP are also involved in m⁶A writing. Human KIAA1429 (Schwartz *et al.*, 2014), a homologue of *Drosophila melanogaster* Virilizer (Vir) (Niessen *et al.*, 2001), associates with METTL3 and is required for m⁶A writer activity in mammals. Vir was first isolated as a factor that, together with the *D. melanogaster* orthologue of WTAP (Fl(2)D) regulated sex determination (Hilfiker *et al.*, 1995; Niessen *et al.*, 2001; Ortega *et al.*, 2003). Despite sharing many common features with the mammalian methylation process, yeast does not have a homologue of KIAA1429, but an additional protein, SLZ1 (Sporulation-specific Leucine Zipper 1), absent in humans, is in the yeast complex and is necessary for mRNA methylation activity (Agarwala *et al.*, 2012).

Until now, no orthologues of METTL14 and KIAA1429 have been shown to be required for m⁶A writing in organisms distinct from mammals (Meyer & Jaffrey, 2014; Fray & Simpson, 2015; Yue *et al.*, 2015). In *S. cerevisiae*, a physical association between IME4 (homologue of METTL3) and KAR4 (homologue of METTL14) has been reported (Ito *et al.*, 2001). However, yeast KAR4 lacks a characteristic S-adenosyl methionine binding domain and thus it is likely to perform a different role to mammalian METTL14 (Bujnicki *et al.*, 2002; Lahav *et al.*, 2007).

Here we report the identification of a conserved set of proteins forming the m⁶A writer complex in *Arabidopsis*. They include MTA (orthologue of human METTL3), MTB (METTL14), FIP37 (WTAP) and VIRILIZER and a homologue of human HAKAI. HAKAI was first characterized in humans as a RING domain E3 ubiquitin-ligase that mediates the post-translational downregulation of E-cadherin at the plasma membrane (Fujita *et al.*, 2002). It has recently appeared in animal proteomics interaction lists that include other m⁶A writer complex members (Horiuchi *et al.*, 2013); however, until now, a role in m⁶A writing has not been proposed. The demonstration here – that this interaction is conserved across kingdoms and that plant HAKAI is functionally required for full mRNA methylation – may indicate that a similar role for mammalian HAKAI should also be considered.

Materials and Methods

Plant growth conditions

Seeds were surface-sterilized and, after 2 d of stratification at 4°C, cultivated under a 16 h : 8 h photoperiod, 22 : 18°C, light : dark, on 0.5 × Murashige & Skoog medium with 1% sucrose, unless indicated otherwise. For anatomical, histological and reporter gene analyses, primary roots of 4–6-d-old vertically grown seedlings were used. Inducible transgene expression was controlled by germinating seeds for 6 d (together with appropriate controls) on sterile media containing 5 µM 17-β-estradiol (est) (purchased from Sigma) and documented. In adult plants, 20 µM est was sprayed every other day after rosette formation.

Plant strains

All *Arabidopsis thaliana* (L.) Heynh. lines were in the Columbia (Col-0) accession. The following mutants and transgenic plants were described previously: *AHP6prom:GFP* (Mähönen *et al.*, 2006), *35Sprom:SR34-RFP* (Lorković *et al.*, 2008) and *ABI3prom:MTA* complemented *mta* SALK_074069 allele (Bodi *et al.*, 2012). The T-DNA insertion SALK_018636 (*fip37-4*) line was obtained from the NASC Stock Centre (Nottingham, UK) and GABI_217A12 (*hakai-1*) from GABI-Kat (Bernd Weisshaar, Bielefeld, Germany) (Kleinboelting *et al.*, 2012). The construct for the CRISPR mutagenesis of *hakai-2* was made by Golden Gate cloning (New England Biolabs, Hitchin, UK) using the vectors and methods described previously (Nekrasov *et al.*, 2013). It was designed to make the sgRNA GATTACGGTGGTGGGAGTCA, which targets a site in the first coding exon. Following transformation, T1 plants were initially screened for the presence of an *Mhl*I resistant *HAKAI* PCR product and putative homozygous disruption lines were further confirmed by sequencing. Lines homozygous for the *hakai-2* mutation, but lacking the Cas9 T-DNA were selected from subsequent generations.

DNA manipulations and transgenic work

The *vir-1* phenotype rescuing *VIRprom:GFP-VIR* was derived from a genomic sequence comprising 2155 bp of the *VIR*

promoter region which was fused with GFP in pEPA vector (Ruzicka *et al.*, 2010), and subcloned into pML-BART binary vector (Gleave, 1992). *35S_{prom}:GS-VIR* was constructed from *VIR* genomic sequence in pDONR221 recombined into pKNGSTAP (Karimi *et al.*, 2007) by a standard Gateway procedure (Invitrogen). MTB, FIP37 and HAKAI mCherry Multisite Gateway based C-terminal fusions were made as previously described (Karimi *et al.*, 2007) and according to the manufacturer's instructions (Invitrogen), using 2374, 1823 and 1680 bp of their native promoter regions, respectively.

The β -estradiol inducible transgene *WOL_{prom}:XVE>>VIR* RNAi and *UBQ10_{prom}:XVE>>MTB* RNAi constructs were made as described previously (Mähönen *et al.*, 2014; Siligato *et al.*, 2016), inserting the regions detailed in Table S1 (Supporting Information) (table of primers used) in the sense and antisense orientation into entry clones with restriction enzyme-mediated cloning. The promoter *UBQ10* was chosen because it directs stable, widespread expression and is resistant to silencing (Geldner *et al.*, 2009). The empty RNAi hairpin was used as a negative control.

Tandem affinity purification

Cloning of transgenes encoding tag fusions under control of the constitutive cauliflower mosaic virus 35S promoter and transformation of *Arabidopsis* cell suspension cultures were carried out as described previously (Van Leene *et al.*, 2007). Two independent tandem affinity purifications of protein complexes were performed using the GS tag (Van Leene *et al.*, 2008) followed by the GS purification protocol as described in Van Leene *et al.* (2011). The protocols of proteolysis and peptide isolation, acquisition of mass spectra by a 4800 Proteomics Analyzer (Applied Biosystems, Framingham, MA, USA), and MS-based protein homology identification based on the TAIR genomic database, have been described previously (Van Leene *et al.*, 2010). Putative false positive interactions were subtracted based on prior experience with *c.* 40 TAP experiments on wild-type (WT) cultures and cultures expressing TAP-tagged mock proteins GUS, RFP and GFP (Van Leene *et al.*, 2010).

m⁶A analysis

The quantification of relative m⁶A levels was performed as described previously (Zhong *et al.*, 2008). Briefly, 20 μ g of total RNA was extracted from *Arabidopsis* seedling samples (or from roots of β -estradiol treated inducible RNAi lines) using the RNAqueous kit (Ambion), the poly(A)⁺ fraction was purified twice using the MicroPoly(A) Purist kit (Ambion) and the quality of the mRNA checked on an RNA 6000 LabChip, with an Agilent Bioanalyzer (Ambion). For each sample, 50 ng of mRNA was digested with 1 μ l of Ribonuclease T1 (1000 units μ l⁻¹; Fermentas, Altrincham, UK) in a final volume of 10 μ l (1 \times polynucleotide kinase buffer) for 1 h at 37°C and the exposed 5' end of the digested mRNA fragments labelled using T4 polynucleotidekinase (10 units; Fermentas) and 1 μ l [γ -³²P] ATP (6000 Ci mmol⁻¹; Perkin-Elmer, Waltham, MA, USA). Following ethanol

precipitation, labelled RNA was resuspended in 10 μ l of 50 mM sodium acetate buffer (pH 5.5) and digested with P1 nuclease (Sigma-Aldrich) for 1 h at 37°C. 2 μ l of each sample was loaded onto cellulose TLC plates (20 \times 20 cm; Merck, Hertfordshire, UK) and developed in a solvent system consisting of isobutyric acid: 0.5 M NH₄OH (5 : 3, v/v), for the first dimension, and isopropanol : HCl : water (70 : 15 : 15, v/v/v), for the second dimension. Spot intensities were determined using a storage phosphorscreen (K-Screen; Kodak, Rochester, NY, USA) and Bio-Rad Molecular Imager FX in combination with QUANTITY ONE 4.6.3 software (Bio-Rad).

Seedling phenotype analysis

For the quantification of seedling phenotypes, the plates with seedlings were photographed and measured with IMAGEJ software (Schneider *et al.*, 2012). Vertical growth index, as a measure of gravitropic response, defined as a ratio between the root tip ordinate and the root length, was determined as described previously (Grabov *et al.*, 2005). Approximately 15–20 seedlings were processed for each treatment, and three independent experiments were performed, giving the same statistically significant results (representative experiments are presented).

For statistical analysis, equal variances of datasets were verified by the Levene test, and the Kruskal–Wallis nonparametric test was performed simultaneously with ANOVA. Data were evaluated with NCSS 2007. The data presented are means \pm standard errors.

Histological analysis and microscopy

Fuchsin staining and confocal imaging were performed on the primary roots of 4–5-d-old seedlings as described previously (Mähönen *et al.*, 2006). The quantitative analysis of protoxylem phenotypes was performed on fuchsin-stained roots as described (Bishopp *et al.*, 2011). Lugol staining for columella starch granules was carried out as described previously (Friml *et al.*, 2002). For the confocal laser scanning microscopy, a Zeiss LSM 780 microscope was used. Due to low signal intensity of transgenes inside the root stele, the contrasts and brightness were enhanced to reveal expression and localization patterns, unless stated otherwise. The analysis of *AHP6_{prom}:GFP* on longitudinal optical sections were acquired with the same confocal settings on all lines in the experiment and the (heat map) RAINBOWRGB lookup table was applied on unprocessed images by IMAGEJ in order to demonstrate expression changes (Schneider *et al.*, 2012).

Genetic screening and positional cloning

The *vir-1* mutant was isolated in an EMS mutagenesis screen for altered pattern of *AHP6_{prom}:GFP* expression. The 970-kb mapping window between marker nga172 and BAC F2O10 on chromosome 3 was established using 100 F₂ recombinant plants. Using Illumina whole genome sequencing (CD Genomics, Shirley, NY, USA; Schneeberger *et al.*, 2009), we identified three mutations within the mapping window in intragenic regions: one in intronic sequence unrelated to known splicing consensus elements, one that

caused a synonymous mutation and one in the 5' splice site of *VIR* intron 5 that led to mis-splicing of *VIR* transcripts.

Sequence analysis and multiple sequence alignment

The domain composition of *VIR* was examined using SMART (Letunic *et al.*, 2012) and Pfam (Punta *et al.*, 2012) databases. For creating the multiple sequence alignments, the protein sequences were aligned using the CLUSTAL OMEGA algorithm (Sievers *et al.*, 2011) and graphically visualized by JALVIEW v.2.8.0b1 using default CLUSTALX colour code (Waterhouse *et al.*, 2009).

RNA sequencing

Three biological replicates each of 5-d-old *vir-1* and the complemented mutant seedlings were harvested directly into RNA stabilizing reagent RNAlater (Ambion). Approximately 1-mm root tips were excized and used as the tissue source for RNA sequencing. Total RNA was extracted with RNAqueous kit (Ambion) and treated with DNase (Fermentas, Thermo Fisher Scientific Fermentas, Vilnius, Lithuania). 1–3 µg of total-RNA was used for isolation of poly(A)⁺ RNA (Dynabeads mRNA purification kit; Ambion). The poly(A)⁺ RNA was reverse-transcribed to cDNA (SuperScript Double-Stranded cDNA Synthesis Kit, Invitrogen Life Technologies, Carlsbad, CA, USA). Random hexamers (New England BioLabs) were used for priming the first strand synthesis reaction and SPRI beads (Agencourt AMPure XP, Beckman Coulter, Brea, CA, USA) for purification of cDNA. Illumina compatible Nextera Technology (Illumina, San Diego, CA, USA) was used for preparation of RNA-seq libraries, employing DNA fragmentation and tagging by *in vitro* cut-and-paste transposition; 60 ng of cDNA was used instead of DNA. After the fragmentation reaction, the fragmented cDNA was purified with SPRI beads. In order to add the Illumina-specific bridge PCR compatible sites and enrich the library, limited-cycle PCR (five cycles) was performed according to the instructions for the Nextera system with minor modifications. For bar-coded libraries, 50 X Nextera Adaptor 2 was replaced with a bar-coded Illumina-compatible Adaptors from the Nextera Bar Codes kit (Illumina) in PCR setup. SPRI beads were used for purification of the PCR products and the library QC was evaluated by Agilent Bioanalyzer (Agilent, Santa Clara, CA, USA).

Each transcriptome was loaded to occupy 1/4 of the lane capacity in a flow cell. C-Bot (TruSeq PE Cluster Kit v3, Illumina) was used for cluster generation and Illumina HiSeq2000 platform (TruSeq SBS Kit v3 reagent kit) for paired-end sequencing. Each biological replicate was sequenced once, producing 100 bp paired-end reads that were then quality trimmed to a length of 93 bp. The sequencing resulted in *c.* 113 M and *c.* 123 M reads for the complemented *vir-1* line and *vir-1*, respectively. The sequencing was done in collaboration with the Finnish Institute for Molecular Medicine, Helsinki, Finland.

Transcriptome analysis

For testing the effects of *vir-1* on global splicing with rMATS (v.3.2.5; Shen *et al.*, 2014), the obtained quality filtered reads in

FASTQ format were trimmed to 80 nucleotides using the rMATS TRIMFASTQ Python script. The trimmed reads were then aligned to the TAIR10 genome build using STAR (Dobin *et al.*, 2013). The WT and *vir-1* data were compared using the *-c* parameter set to 0.0001 (0.01% splicing difference). Summary outputs filtered by FDR ($Q < 0.05$) from rMATS are provided (Table S2).

For analyses based on differential expression, sequences were aligned against the TAIR10 genome using TOPHAT (v.2.0.8b) with the options *-bowtie1* and *-no-discordant* in two runs and a mean inner distance between mate pairs of 112 to 133 (SD = 50). The junctions predicted by the first run supplied to the second run. Transcript counts were calculated with HTSEQ with features marked in the ENSEMBL v.72 TAIR10 Gene Transfer Format annotation. Differential gene expression was assessed with the DESEQ package (Anders & Huber, 2010). The full procedure is described in (Edgren *et al.*, 2011). The GO analysis of complete gene list expressed in the *vir-1* root tip was done using the AGRIGO tools (Du *et al.*, 2010) with FDR-corrected *P*-value (*Q* value) as a ranking criterion and Hypergeometric test (Hochberg FDR) with 0.05 significance cut-off. The list of vascular regulators (Caño-Delgado *et al.*, 2010) has been used as a benchmark for defining appropriate GO terms for generating manually edited and updated list of genes required for vascular formation.

Quantitative RT-PCR

Quantitative reverse transcription polymerase chain reaction (qRT-PCR) was carried out as described previously (Furuta *et al.*, 2014) using a LightCycler 480 (Roche) with LightCycler 480 SYBR Green master mix (Roche) and the manufacturer's qRT-PCR program recommendations. Four technical repeats were carried out to assess the gene expression levels. Gene expression was normalized to *UBQ10*, as described previously (Furuta *et al.*, 2014).

Yeast two-hybrid system

The protein–protein interactions were tested as described previously (Zhong *et al.*, 2008; Pekárová *et al.*, 2011). Plasmids were constructed by Gateway-based technology using destination vectors pDEST22 (activation domain) and pDEST32 (binding domain). *VIR* sequence was split into two parts, corresponding to amino acid residues 1 to 2883 (part 1) and 2584 to 6417 (part 2), referring to the AT3G05680.1 gene model. The interactions were tested in three technical and three biological replicates on media lacking histidine and supplemented with inhibitor of histidine synthesis, 3-amino-1,2,4-triazole (3-AT; Sigma). The yeast growth was recorded after 4 d.

Accession numbers

Sequence data for genes described in this article can be found in the Arabidopsis Genome Initiative or GenBank/EMBL databases under the following accession numbers: *AHP6* (At1g80100), *MTA* (At4g10760), *MTB* (At4g09980), *FIP37* (At3g54170),

VIR (At3g05680) and *HAKAI* (At5g01160). The raw sequences for *vir-1* transcriptome and rMATS outputs have been deposited in the Gene Expression Omnibus (GEO) database, accession GSE97174.

Results

Identification of a viable mutant orthologous to the splicing regulator/m⁶A writer protein VIRILIZER/KIAA1429

The histidine pseudophosphotransmitter AHP6 is a factor required for protoxylem formation in *Arabidopsis* and is the earliest marker of root protoxylem development (Mähönen *et al.*, 2006). In a mutant screen designed to identify regulators of *Arabidopsis* vascular development, we isolated one line that exhibited reduced and irregular *AHP6**prom:GFP* expression (Fig. 1a) accompanied by defects in protoxylem development in the primary root (Fig. 1b). We used positional cloning and whole genome sequencing to identify *EMB2016* (Tzafrir *et al.*, 2004) as the disrupted gene (Fig. 1c). This gene of unknown function was described previously as essential (Tzafrir *et al.*, 2004) and is homologous to the *D. melanogaster* sex determination splicing factor, Virilizer (Hilfiker *et al.*, 1995; Niessen *et al.*, 2001), and to human KIAA1429, associated with m⁶A formation in mammals (Schwartz *et al.*, 2014; Fig. S1). Based on the homology to the prototypical gene, we refer to this mutant (and gene) as *virilizer-1* (*vir-1*). The *vir-1* EMS-induced mutation results in a G-to-A conversion at the first nucleotide of intron 5, leading to numerous predominantly wrongly spliced *VIR* transcripts with minor but detectable content of the correct *VIR* mRNA (Figs 1c–e, S2a). The *vir-1* mutant exhibited pleiotropic phenotypes, which included aberrant root cap formation, gravity response and lateral root development, as well as defective cotyledonal development (Fig. S2b–f). Because these aberrant phenotypes were rescued by complementation with a *VIR* (Figs 1f, S2g), and phenocopied by inducible *VIR* RNAi lines (Fig. S2h), we concluded that we had isolated a viable hypomorphic *virilizer* allele.

Transcriptome of *vir-1* mutant

Drosophila melanogaster Vir is required for promoting certain alternative splicing events associated with female gametogenesis and X chromosome dosage compensation (Hilfiker *et al.*, 1995; Ortega *et al.*, 2003; Haussmann *et al.*, 2016; Lence *et al.*, 2016). We isolated poly(A)⁺ RNA from *vir-1* root tips and carried out Illumina RNA sequencing. We examined the changes in alternative splicing in *vir-1* using rMATS tools (Shen *et al.*, 2014). Only 22 retained introns, one mutually exclusive exon, and eight skipped exon, one alternative 5' and 13 alternative 3' splice sites (FDR < 0.01) were identified (Table S2). Given the selected threshold (see the Materials and Methods section), we conclude that the *vir-1* mutation does not result in extensive alternative or mis-splicing of transcripts.

Gene ontology (GO) analysis (Du *et al.*, 2010) based on the differentially expressed genes in the *vir-1* mutant (Table S3)

revealed that the *vir-1* mutation affects a range of processes which include those associated with response to environmental cues, metabolic processes and macromolecular localization, and also growth and development (Table S4). The root tip tissue-specific context allowed us to examine expression of early vascular genes (Table S5). Out of 138 vascular formation related genes identified in our dataset, 35 have been misexpressed, which suggests that vascular development in *vir-1* is affected at multiple levels (Table S6). Altogether, the observed changes in the *vir-1* root tip transcriptional profiles suggests that *VIR* is likely involved in regulation of gene expression, but the function of *VIR* is rather general than specific and knock-down of *VIR* does not affect overall splicing rates in *Arabidopsis*.

VIR closely associates with a conserved set of proteins linked with m⁶A writing

Although it is a relatively large protein (236 kDa), *VIR* lacks well-characterized protein domains and its precise molecular function remains obscure. The mammalian homologue of *VIR* was recently shown to associate with m⁶A writer proteins (Ortega *et al.*, 2003; Horiuchi *et al.*, 2013; Schwartz *et al.*, 2014), we therefore decided to test experimentally whether a similar association also existed in *Arabidopsis*. We used tandem affinity purification (TAP) followed by proteolysis and mass spectrometry (Van Leene *et al.*, 2011) to identify proteins that associated with the *VIR*-GS bait in *Arabidopsis* suspension cell cultures. Using this approach, we consistently identified FIP37 (Zhong *et al.*, 2008) and *HAKAI* (Fig. S3; Fujita *et al.*, 2002; Horiuchi *et al.*, 2013) co-purifying with *VIR* and MTB (Bujnicki *et al.*, 2002) also significantly enriched with a lower confidence score (Fig. 2a; Table S7).

In order to further characterize these putative members of the m⁶A writer complex and to examine their relationship to the known plant m⁶A methylase MTA, we tested several pairwise interactions between them using the yeast two-hybrid system (Y2H) (Fig. 2b). In addition to the known MTA-FIP37 interaction (Zhong *et al.*, 2008), we observed heterodimerization of the *Arabidopsis* MTA and MTB, consistent with the reported interaction between their mammalian orthologues METTL3 and METTL14 (Liu *et al.*, 2014; Ping *et al.*, 2014; Wang *et al.*, 2014b). We also found that MTB but not MTA formed homodimers in Y2H. These data support the findings of Liu *et al.* (2014) who reported that mammalian methylases METTL3 and METTL14 can form heterotetramers. In addition, FIP37 also gave self-interaction and a consistent though weaker interaction was also seen between *HAKAI* and MTB. Due to lower interaction fidelities of very large proteins in Y2H (Koegl & Uetz, 2007), we split *VIR* protein into two parts and also used it for Y2H. However, no interaction was seen with the N-terminal fragment and only strong transactivation or no interaction was seen with the carboxy terminal fragment in our test system (Fig. 2b). In summary, we show that, in addition to MTA and FIP37 (Zhong *et al.*, 2008), MTB, *VIR* and *HAKAI* are also associated in the *Arabidopsis* m⁶A writer complex.

Because this conserved set of associating proteins co-purify, one would expect that they would be found together in the same cell

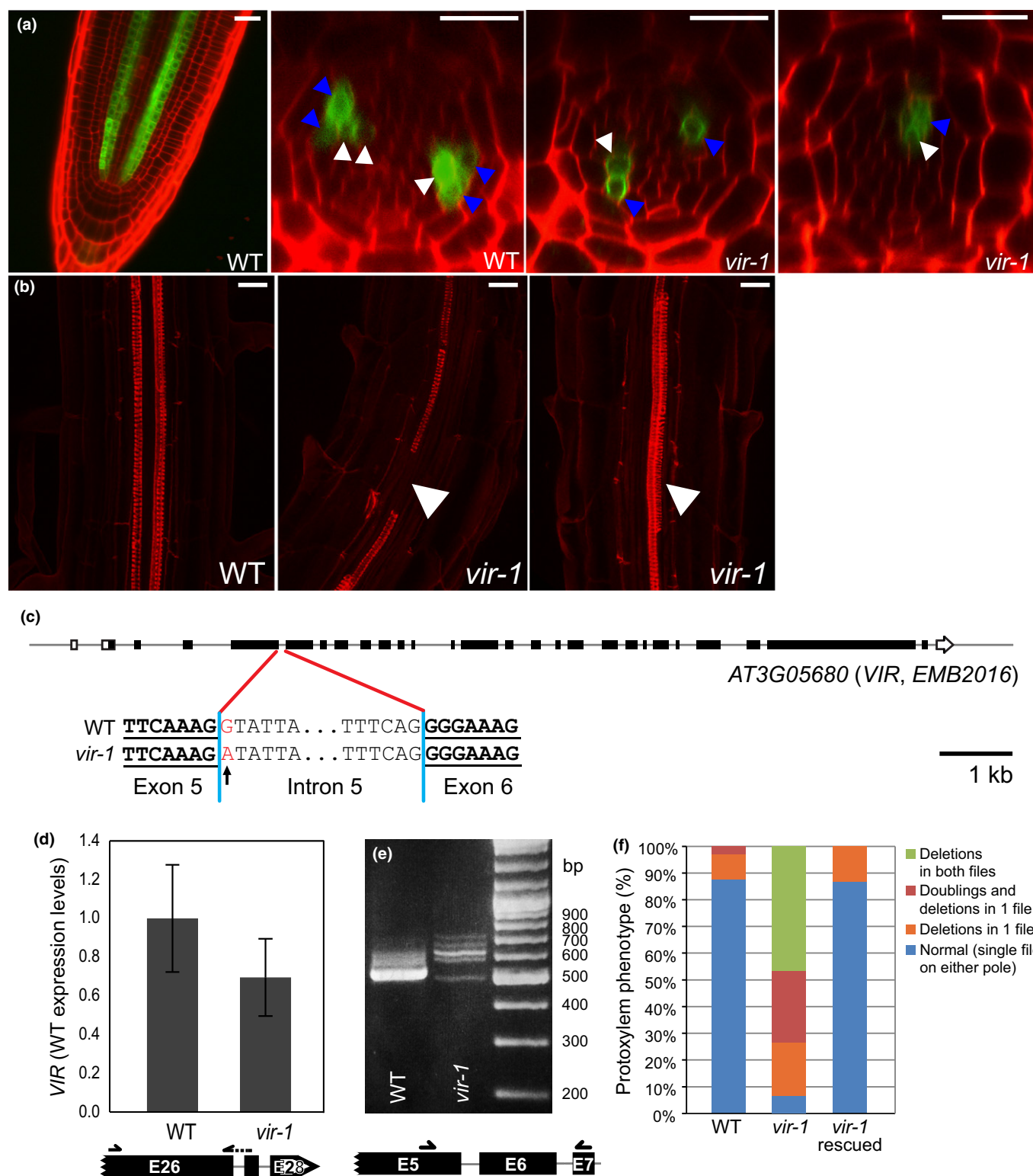


Fig. 1 A hypomorphic mutation in the *VIRILIZER* (*VIR*) locus of *Arabidopsis thaliana* leads to vascular defects. (a) Wild-type (WT) expression pattern of the *AHP6**prom::GFP* marker in the root protoxylem founder cells and its aberrant expression in *vir-1*, as documented by optical longitudinal and cross-section images. In the WT, the reporter is expressed in one or two files on each side inside the vascular cylinder (giving rise to protoxylem, white arrowheads) and in two accompanying cells of pericycle (blue arrowheads). (b) Fuchsin staining illustrating *vir-1* protoxylem defects, such as interruptions or doubling of protoxylem (arrowheads). (c) The *vir-1* mutation is caused by a single nucleotide substitution in the 5' splice site of the 5th intron of the *VIR* gene. Although the *vir-1* mutation does not significantly change *VIR* expression levels at $\alpha_{0.05}$ (d), it affects its correct splicing as assayed by reverse transcription polymerase chain reaction (RT-PCR) around mutated site in *vir-1* (e). (f) Quantification of the *vir-1* protoxylem phenotype, which can be rescued by introducing a *GFP-VIR* transgene into *vir-1* plants. Quantitative RT-PCR (d) data are represented as means \pm SE. Bars, 20 μ m.

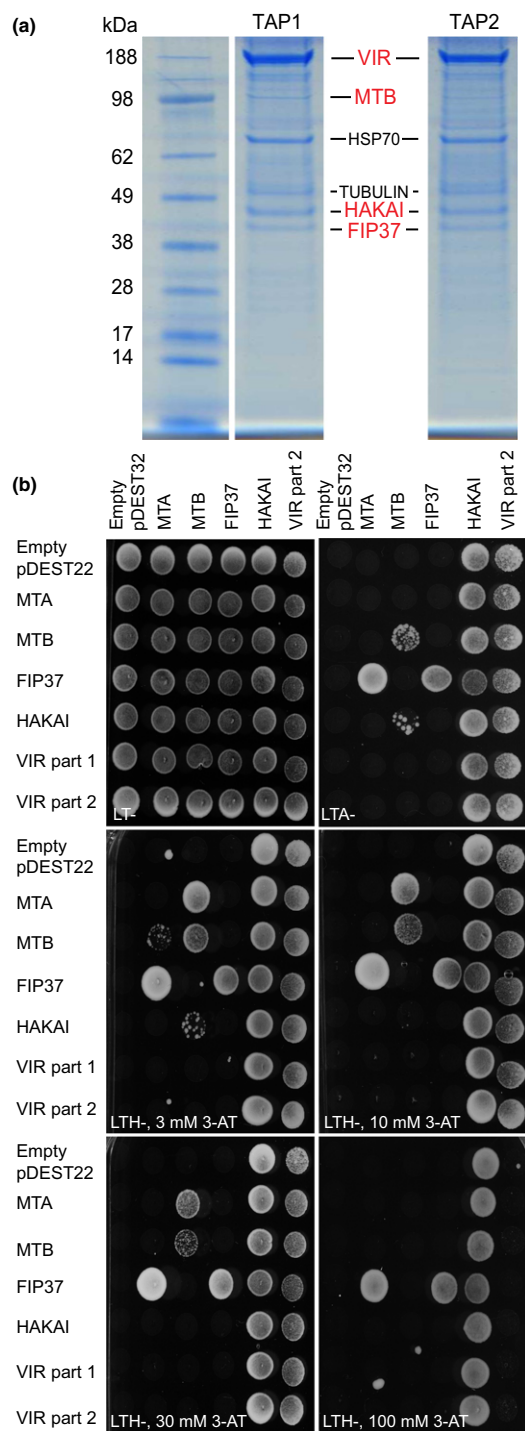


Fig. 2 VIRILIZER (VIR) associates with m⁶A writer proteins in *Arabidopsis thaliana*. (a) In tandem affinity purification (TAP), VIR (bait) co-purifies with FIP37 and HAKAI and in replicate 1 also with the putative N⁶-adenosyl methylase MTB; TAP1 and TAP2 are two independent TAP experiments; HSP70 and TUBULIN were considered as nonspecific binding proteins, as described in the Materials and Methods section. (b) In the yeast two-hybrid assay, putative writer proteins fused to activation (pDEST22 vector) and binding (pDEST32 vector) domains show pairwise interactions under various stringency conditions – as documented by growth on selective media lacking with leucine, tryptophan and histidine (-LTH) and supplemented with various concentrations of 3-AT to balance basal expression of the *HIS3* reporter, or lacking leucine, tryptophan, and adenine (-LTA).

types. To address this question with a complementary approach, we used confocal microscopy to examine the localization of each protein fused with mCherry fluorescent tag, stably transformed into a line expressing a functional *VIRprom::GFP-VIR* construct (Fig. 1f). In each case, the native promoters were used to drive the expression of the coding sequences of the fusion proteins. We first characterized the GFP-VIR fluorescence. The signal was detected in the nucleoplasm of all root tip cell types (Figs 3, S4). There was no clear fluorescence indicative of enriched localization of GFP-VIR in nucleoli, the cytoplasm or in foci resembling (pro)plastid organelles (Fig. 3). In the root meristem nuclei, the GFP-VIR showed an even signal distribution (Fig. 3c), whilst the differentiated cells above the root elongation zone exhibited a punctate nuclear distribution pattern (Fig. 3d), similar to known splicing factors (Fang *et al.*, 2004; Tillemans *et al.*, 2006). In order to test the idea that this punctate pattern might indeed correspond to splicing speckles, we crossed the GFP-VIR plants with lines stably expressing splicing protein SR34 fused to RFP (Lorković *et al.*, 2008). The observed co-localization of SR34-RFP and GFP-VIR indicates that the GFP-VIR can localize to splicing speckles (Fig. 3d). Finally, the expression pattern of each protein associating with VIR, MTB (Fig. 3e), FIP37 (Fig. 3f) and HAKAI (Fig. 3g) -mCherry overlapped with GFP-VIR in all tissues examined in *Arabidopsis* root tips (Figs 3e–g, S4).

The merged fluorescent signals in each combination examined reveal that these proteins are found within close proximity in both dividing and differentiated *Arabidopsis* cells. This is consistent with the *in vivo* interaction proteomics data and suggests that they interact functionally and physically.

Establishing a set of stable transgenic lines that perturb the expression of the proteins associated with m⁶A writing

In order to test the requirement for each of the associating proteins in writing m⁶A, we generated a collection of *Arabidopsis* lines defective in the expression of MTB, FIP37, VIR and HAKAI (Figs 1b–d, 4). Null mutations in *MTA* are embryonic lethal (Zhong *et al.*, 2008), as are null alleles of *Arabidopsis* *MTB*, *FIP37* and *VIRILIZER* (Tzafrir *et al.*, 2004; Vespa *et al.*, 2004). However, we identified a viable hypomorphic allele of *FIP37*, caused by a T-DNA insertion within its 7th intron (*fip37-4*, identical to that described in Shen *et al.* (2016); Fig. 4a). We also identified an insertion mutant of *hakai* (*hakai-1*; Fig. 4b), and generated a deletion *hakai* allele using CRISPR/Cas9 to remove a single nucleotide in the coding sequence of the 1st exon (*hakai-2*, Fig. 4b). All of these homozygous mutants were viable in our growth conditions. qRT-PCR confirmed that expression of the respective genes was compromised in each case (Fig. 4c).

We also constructed inducible RNAi lines (Mähönen *et al.*, 2014) to knockdown the expression of *MTB* and used RT-qPCR to confirm that expression was knocked-down upon addition of the inducer β -estradiol (Fig. 4d). In summary, we have developed a set of viable genotypes that partially or completely disrupt the expression of genes encoding each of the putative m⁶A writers. These provide a genetic resource to analyse the functional role of MTB, FIP37, VIR and HAKAI in writing m⁶A.

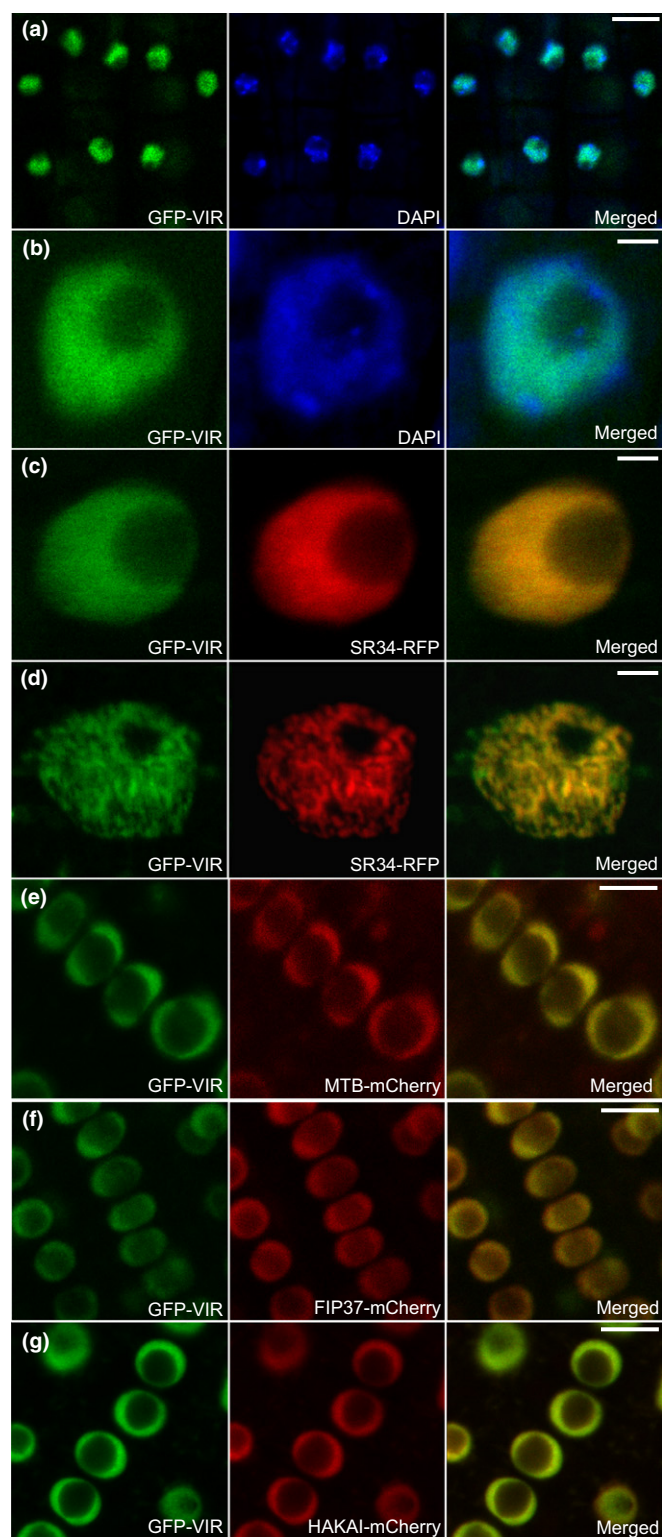


Fig. 3 *Arabidopsis thaliana* proteins linked with m⁶A writer activity are nuclear localized. (a, b) GFP-VIR co-localizes with fluorescent DNA-binding dye DAPI. (c, d) GFP-VIR co-localizes with nuclear localized splicing factor SR34-RFP. Smooth nuclear fluorescence distribution was seen in the root tip (c), the characteristic punctate subnuclear compartments (splicing speckles) were observed in the differentiated cells above the root elongation zone (d). (e–g) GFP-VIR co-localizes with MTB (e), FIP37 (f) and HAKAI (g) fused to mCherry in root-tip nucleoplasm. Bars: (a, e–g) 10 µm; (b–d) 2 µm.

HAKAI and putative *Arabidopsis* m⁶A writers are required for methylation of mRNA

We next examined the requirement of each protein factor in writing m⁶A to *Arabidopsis* mRNA. We therefore measured the levels of m⁶A in each of the lines. Following two rounds of poly(A)⁺ RNA purification, mRNA was digested with RNase T1 (which cleaves after every G residue). Fragments were then end-labelled using [γ -³²P]ATP and digested to mononucleotides. These were separated and the m⁶A:A ratios determined as described previously (Fig. 5a; Zhong *et al.*, 2008). We found that levels of m⁶A were reduced to 5–15% WT levels in the *fip37-4*, and *vir-1* lines and by 50% in the MTB RNAi line after β -estradiol treatment (Fig. 5b–e). Furthermore, in both *hakai* mutants m⁶A levels were reduced by 35% (Fig. 5f,g). We therefore conclude that each of the newly identified factors, MTB, FIP37, VIR and HAKAI, is required to write WT levels of m⁶A in *Arabidopsis* mRNA.

Genetic depletion of total m⁶A pools leads to similar phenotypic consequences

If MTA, MTB, FIP37, HAKAI and VIR function together to write m⁶A, then it would be expected that mutants defective in these components might share similar developmental defects. Indeed, the *mta*, *mtb*, *fip37* and *vir* null alleles arrest at the globular stage of embryonic development (seedgenes.org; Tzafrir *et al.*, 2004), but both *hakai* alleles are viable (Fig. 6a). Hypomorphic mutants and knockdown lines of these factors or null *mta* mutants rescued by embryo-specific expression of MTA driven by the *ABI3* promoter (*mta ABI3prom:MTA*) (Bodi *et al.*, 2012), show reduced root growth and aberrant gravitropic responses (Fig. 6a–d), whereas both *hakai* alleles rather resemble WT. This distinction may reflect the different impact on global m⁶A levels of these lines, because in each hypomorphic mutant of *MTA* (Bodi *et al.*, 2012), *FIP37* and *VIRILIZER*, m⁶A levels were reduced to a greater extent than in both *hakai* alleles (Fig. 5). In addition, the lines with reduced *MTA*, *MTB*, *FIP37* and *VIR* expression also show delayed development and reduced apical dominance in the generative phase of development, whereas *hakai* mutants more closely resembled WT with respect to these traits (Fig. 6e,f). Because we isolated the viable *vir-1* allele in the course of a screen for factors mediating the regulation of *AHP6prom:GFP* in early stages of root development, we also looked at these traits in more detail. Like the *vir-1* allele which shows a misexpression of *AHP6prom:GFP*, we found that *MTB* knockdown lines and *fip37-4* mutants also showed reduced expression of the *AHP6prom:GFP* reporter (Fig. 7a,b). Importantly, all mutant and knock-down lines show defects associated with vascular development. Similar to *vir-1*, each line exhibits defective protoxylem development, with increased occurrence of interruptions in, and doublings of, protoxylem strands being detected compared to WT (Fig. 7c). In conclusion, all mutants share defects in vascular development and reductions of m⁶A. Embryonic lethality of null alleles and other developmental defects are shared in hypomorphic lines defective in MTA, MTB,

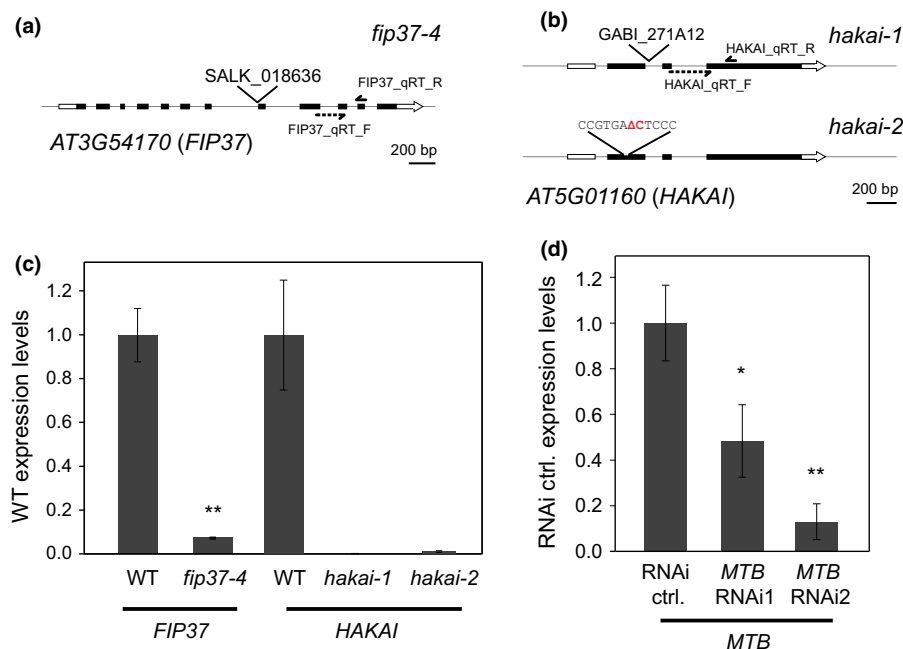


Fig. 4 Molecular properties of transgenic lines with depleted expression of proteins associated with *Arabidopsis thaliana* writer proteins. (a) T-DNA insertion mutant line SALK_018636 is a weak *fip37-4* allele. (b) *hakai-1* (GABI_271A12) is an insertional and *hakai-2* is a CRISPR/Cas9-derived 1-bp deletion allele in the *HAKAI* gene. (c) *fip37-4*, *hakai-1* and *hakai-2* show strongly depleted levels of their respective transcripts as determined by quantitative reverse transcription polymerase chain reaction (qRT-PCR), in *hakai* alleles, the amounts of *HAKAI* transcript dropped below detection limits of the instrument. (d) Reduced expression of *MTB* was also observed in inducible *UBQ10prom: XVE>>MTB* RNAi lines. Data are means \pm SE; *, $P < 0.05$; **, $P < 0.01$ by ANOVA. The positions of the primer binding sites are depicted on the gene diagrams, where applicable. For the *MTB* RNAi line and the corresponding control, plant material was grown on media supplemented with 5 μ M β -estradiol.

FIP37 and VIR function, but these are generally less pronounced in *hakai* mutants.

hakai mutants act synergistically with other m⁶A writer mutants

Given the relatively weak *hakai* mutant phenotypes compared to the severe developmental defects seen in the hypomorphs of the other m⁶A writer-associated proteins, we sought to test whether HAKAI also interacted genetically with other writer components. First, we crossed both *hakai-1* and *hakai-2* to the *mta ABI3prom:MTA* line (Bodi *et al.*, 2012) and selected double homozygous mutant plants from the subsequent filial generations. In both cases, the introduction of the *hakai* mutant into the *mta ABI3prom:MTA* hypomorph background gave rise to plants with a compromised growth phenotype that was far more severe than either parent (Fig. 8). m⁶A levels showed a further slight reduction in m⁶A relative to the *mta ABI3prom:MTA* parent (Fig. S5). Next we crossed the *hakai-2* mutant to the *fip37-4* hypomorph and selected plants that were homozygous for *fip37-4* and heterozygous for *hakai-2* from the F₂ generation. These plants were selfed and the F₃ seed planted on Murashige & Skoog media and the emerging seedlings genotyped with respect to the *hakai-2* mutation. Of 73 progenies, 23 (31.5%) were found to be WT with respect to *hakai-2* and 50 (68.5%) were heterozygous. No homozygous *hakai-2* seedlings were found. This suggests that the combination of the *fip37-4* and *hakai-2* mutations

is lethal; indeed the WT:heterozygotes observed ratio is close to the 1:2 that would be predicted if this were the case. We did not observe an increase in the number of nongerminating seeds, suggesting that the double mutants aborted very early in their development.

Discussion

Role of m⁶A in plant development

A regulatory role of N⁶-adenosine methylation (m⁶A) in development and in determining cell fate has been demonstrated in major model systems such as mouse, *Drosophila melanogaster* and *Saccharomyces cerevisiae* (Clancy *et al.*, 2002; Hongay & Orr-Weaver, 2011; Geula *et al.*, 2015; Haussmann *et al.*, 2016). m⁶A has recently been shown to have a crucial role during murine stem cell development, where it prompts stem cell differentiation from their naïve stage (Geula *et al.*, 2015). *Arabidopsis* full knock-outs of MTA, MTB, FIP37 and VIR also do not progress past the embryonic globular stage (Tzafrir *et al.*, 2003; Vespa *et al.*, 2004; Zhong *et al.*, 2008). We have circumvented this embryo lethality by establishing a collection of hypomorphic, mutants or RNAi lines for each of the proteins associated with the m⁶A writer complex in order to study the effects of reduced m⁶A in postembryonic development. In a recently published study, (Shen *et al.*, 2016) reported that reduced FIP37 expression resulted in increased proliferation of the shoot apical meristem.

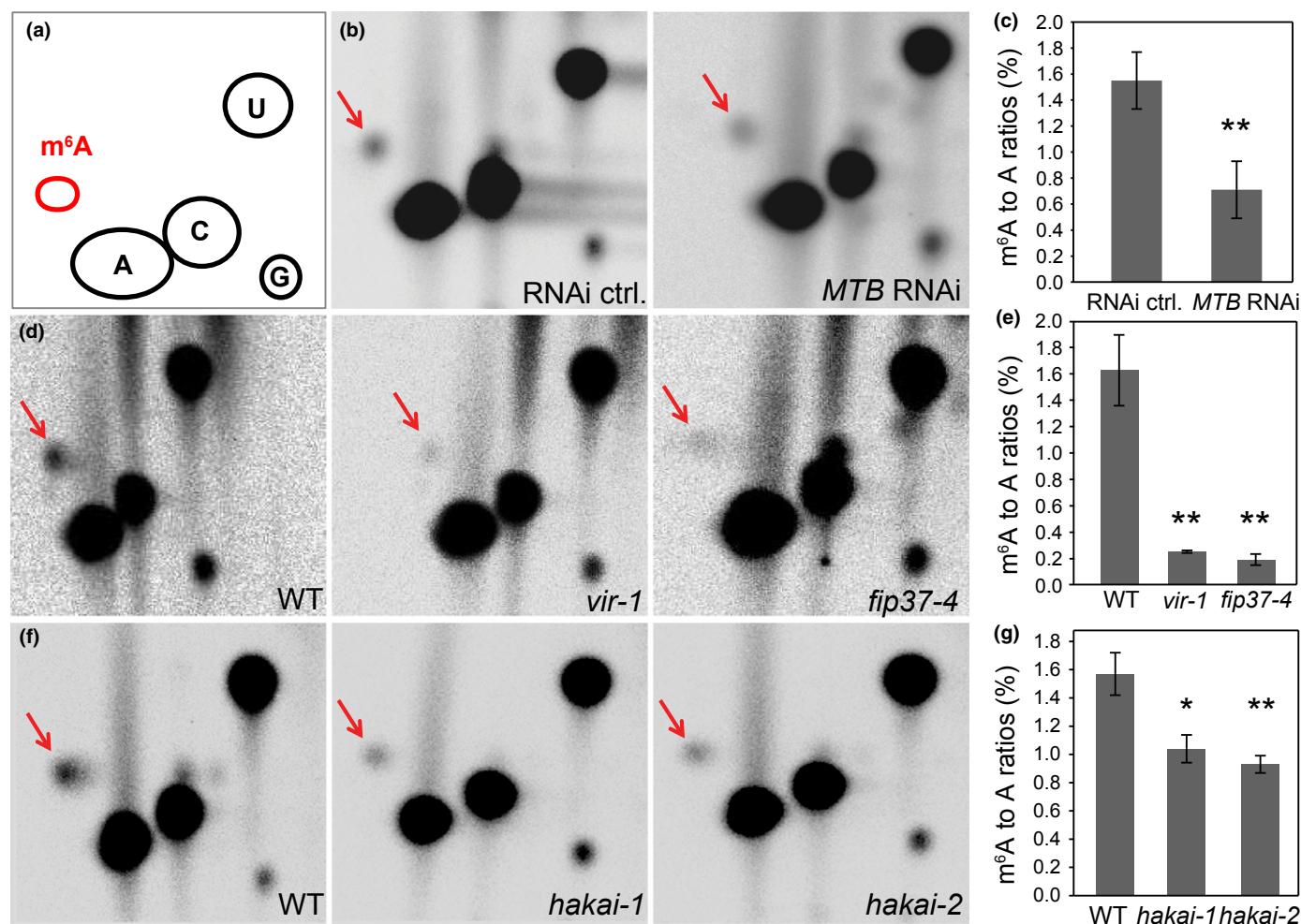


Fig. 5 Proteins associating with the *Arabidopsis thaliana* m⁶A writers are required for methylation of mRNA. (a) Schematic positions of the m⁶A and nonmodified nucleotides separated by 2D thin-layer chromatography. (b, c) m⁶A levels are reduced in poly(A)⁺ RNA of the inducible *UBQ10prom::XVE>>MTB* RNAi lines as shown on the 2D thin-layer chromatogram (b) and quantified from two independent experiments (c). (d, e) Reduced amounts of m⁶A are also seen in poly(A)⁺ RNA of hypomorphic alleles *fip37-4* and *vir-1*. (e) The quantification of three independent replicates carried out on *fip37-4* and *vir-1*. (f, g) The levels of m⁶A are depleted in poly(A)⁺ RNA isolated from *hakai* mutants, as documented by the chromatograms (e) and assessed by three independent replicates for each mutant (g). Data are means \pm SE; *, $P < 0.05$; **, $P < 0.01$ by ANOVA. For the *MTB* RNAi line and the corresponding control, plant material was grown on media supplemented with 5 μ M β -estradiol. Location of the m⁶A spot (b, d, f) is indicated by arrows.

Our findings independently expand this, further revealing that impaired expression of any of the five m⁶A writer components we identify results in a range of developmental defects, including vascular formation, implying a role for m⁶A in establishing and maintaining these processes.

Conserved Eukaryotic writer proteins and role of VIRILIZER

Based on our genetic and biochemical data, we propose that the core constituents of the plant writer complex are nuclear localized proteins MTA, MTB, FIP37, VIR and HAKAI. Orthologues of MTA and MTB interact with each other and with orthologues of FIP37 in *S. cerevisiae* (Agarwala *et al.*, 2012) and human cells (Liu *et al.*, 2014; Ping *et al.*, 2014; Schwartz *et al.*, 2014; Wang *et al.*, 2014b). In *S. cerevisiae*, writing of m⁶A requires orthologues of MTA (IME4), FIP37 (MUM2) and the yeast-specific SLZ1 (Agarwala *et al.*, 2012). In mammals, in addition to the

orthologues of MTA (METTL3) and FIP37 (WTAP), MTB (METTL14) and the splicing/methylation factor VIR (KIAA1429) are also present in the complex and required for m⁶A writing. *Arabidopsis* MTA and MTB are nonredundant and, similar to METTL3 and METTL14 (Liu *et al.*, 2014; Ping *et al.*, 2014; Wang *et al.*, 2014b), they also interact directly in Y2H.

In contrast to *S. cerevisiae*, where the m⁶A writers reside in nucleoli (Agarwala), their plant orthologues occupy the nucleoplasm, similar to animal systems (Bokar *et al.*, 1997; Niessen *et al.*, 2001; Zhong *et al.*, 2008; Liu *et al.*, 2014; Ping *et al.*, 2014). Subnuclear domains, so called nuclear speckles, correspond to sites with active transcription in the interchromatin regions. They are connected with the presence of splicing factors, but less with the accumulation of other factors participating on RNA processing in microscope localization studies (Spector & Lamond, 2011; Reddy *et al.*, 2012). Analogously to their animal orthologues (Liu *et al.*, 2014; Ping *et al.*, 2014), plant writers also

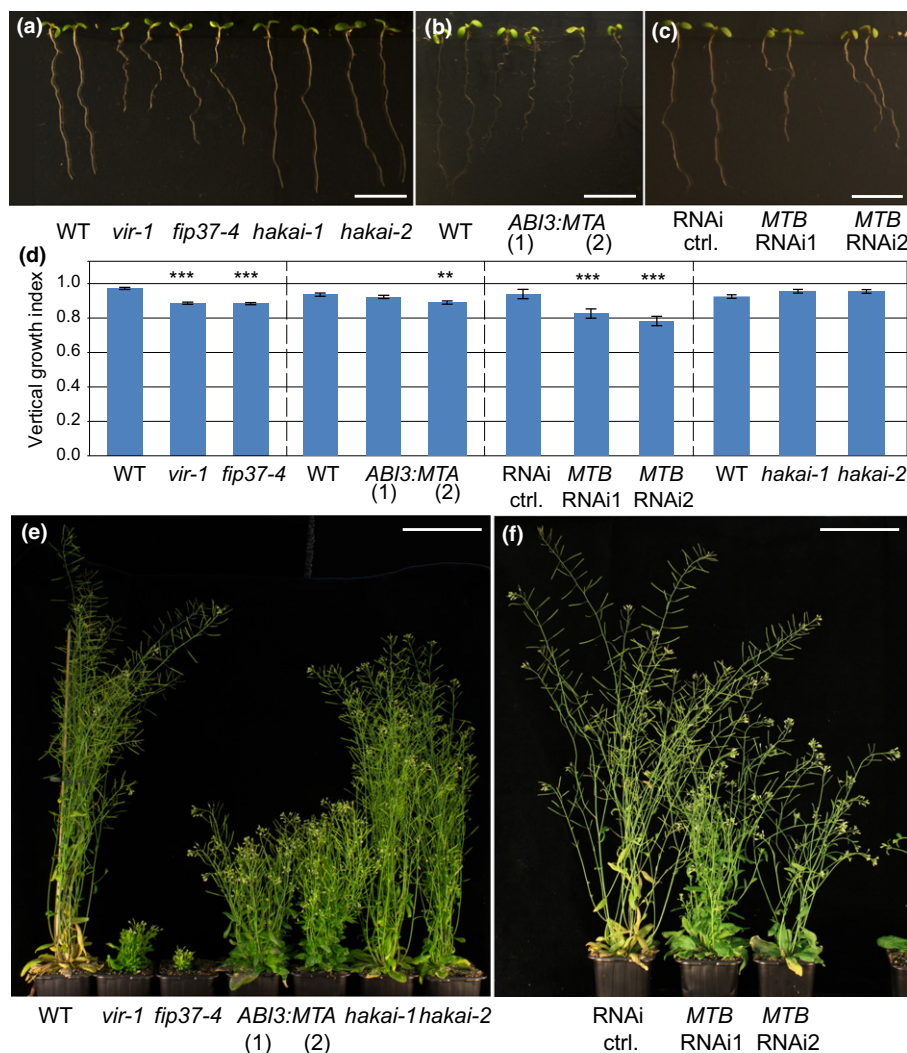


Fig. 6 *Arabidopsis thaliana* lines with defective expression of m⁶A writer proteins exhibit similar phenotypes at the macroscopic level. (a–d) The seedlings of hypomorphic lines *fip37-4*, *vir-1* (a) and *mta ABI3prom:MTA* (two independent lines, marked as *ABI3:MTA*) (b), as well as two independent inducible *UBQ10prom:XVE>>MTB* RNAi lines (c) show similar defects in overall root morphology, whereas both *hakai-1* knockdown and *hakai-2* knockout root growth resemble wild-type (WT) (a); similar trends were seen with in their gravitropic response quantified by vertical growth index (d). (e) Seven-week-old plants with strongly depleted levels of m⁶A show altered generative growth, which includes bushy phenotype and reduced apical dominance, whereas *hakai* mutants rather resemble WT controls. (f) Seven-week-old *UBQ10prom:XVE>>MTB* plants sprayed with 20 μM β-estradiol also show affected generative growth. Bars: (a–c) 10 mm; (e, f) 10 cm. Data are means ± SE; **, *P* < 0.01; ***, *P* < 0.001 by ANOVA. For the *MTB* RNAi seedlings and the corresponding control, plant material was grown on media supplemented with 5 μM β-estradiol.

show a similar punctate pattern (Zhong *et al.*, 2008) and co-localize with the splicing factor SR34-RFP. This splicing factor, as well as the co-localizing writers, shows a more diffuse pattern in the meristematic cells, whereas in the cells above the elongation zone the speckle pattern is more prevalent. This likely coincides with differential transcriptional activities in rapidly dividing and differentiated cells, similar to observations from animal systems (Tillemans *et al.*, 2006; Spector & Lamond, 2011; Reddy *et al.*, 2012). Because m⁶A affects splicing in mammals and *D. melanogaster* (Liu *et al.*, 2014; Ping *et al.*, 2014; Alarcón *et al.*, 2015a; Haussmann *et al.*, 2016; Lence *et al.*, 2016) possibly by recruiting splicing factors (Xiao *et al.*, 2016), it is interesting to speculate whether m⁶A could also regulate splicing in plants. The rather normal splicing patterns observed in *vir-1* root tip suggests that m⁶A is not involved in large-scale regulation of splicing in plants or that splicing regulation only occurs at the transcript or tissue-specific level, which is below the detection limit of the root-tip RNA-Seq.

In yeast, mRNA methylation only occurs naturally under very specific conditions where cells must be diploid and starved for

both a nitrogen and fermentable carbon source (Clancy *et al.*, 2002). In plants and mammals, mRNA methylation amounts vary between different developmental stages or organ types (Zhong *et al.*, 2008; Meyer *et al.*, 2012), indicating that regulation in these multicellular organisms is likely to be more subtle than a simple on or off state. It seems that variations of the writer complex evolved in other eukaryotes. According to our *in silico* analysis, VIR and HAKAI are missing in the genomes of *Fungi*, including *S. cerevisiae*. VIR has been implicated in the regulation of sex-specific alternative splicing in *D. melanogaster* (Hilfiker *et al.*, 1995; Niessen *et al.*, 2001), but more recently it was also found to be required for m⁶A formation in human cells (Schwartz *et al.*, 2014). In *D. melanogaster*, the FIP37 homologue FI(2)D closely associates with VIRILIZER (Ortega *et al.*, 2003) and interacts genetically with methylation pathways to regulate sex-specific splicing events (Haussmann *et al.*, 2016; Lence *et al.*, 2016). In human cells their orthologues WTAP and KIAA1429 also co-purify (Horiuchi *et al.*, 2013; Schwartz *et al.*, 2014). Our data thus indicate that writer proteins in *Arabidopsis* more closely resemble those in mammals than yeast. Our results also highlight

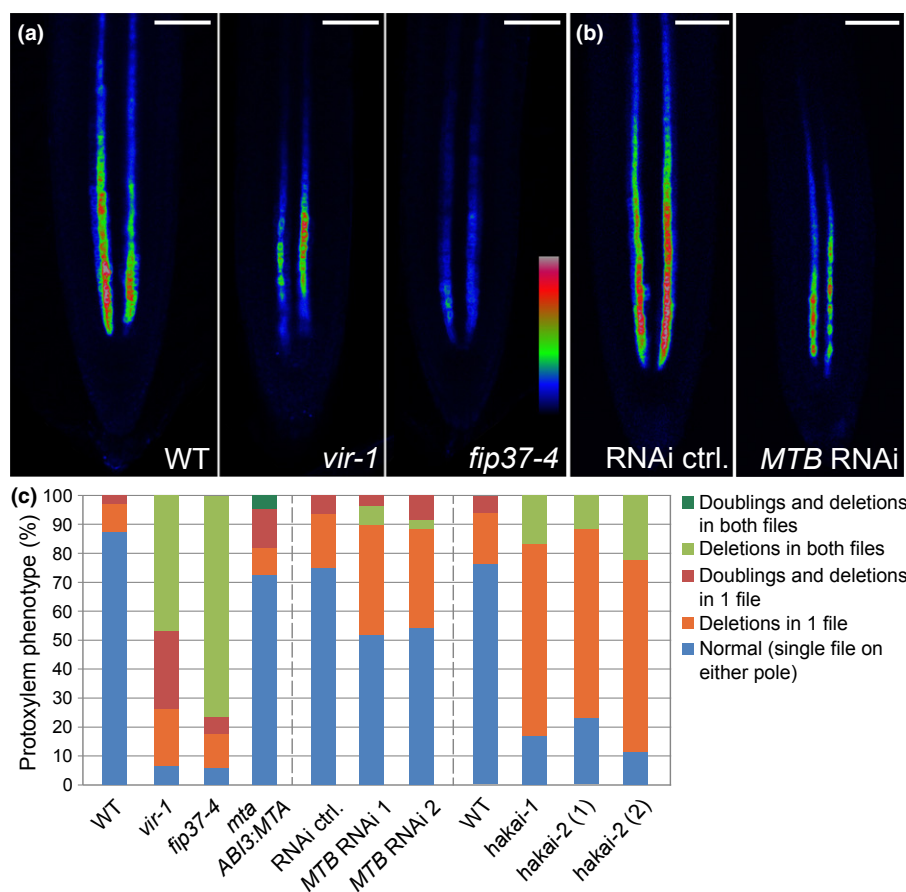


Fig. 7 Reduced expression of proteins associating with the *Arabidopsis thaliana* m⁶A writers results in vascular defects. (a, b) Similar to *vir-1*, *AHP6prom:GFP* fluorescence signal is reduced in the weak *fip37-4* allele (a) and following induction of inducible *UBQ10prom:XVE>>MTB* RNAi (b). (c) Mutants with reduced m⁶A levels show vascular defects, which includes interruptions or duplications of protoxylem files across the primary root. Bars, 50 μ m. For the *MTB* RNAi line and the corresponding control, plant material was grown on media supplemented with 5 μ M β -estradiol.

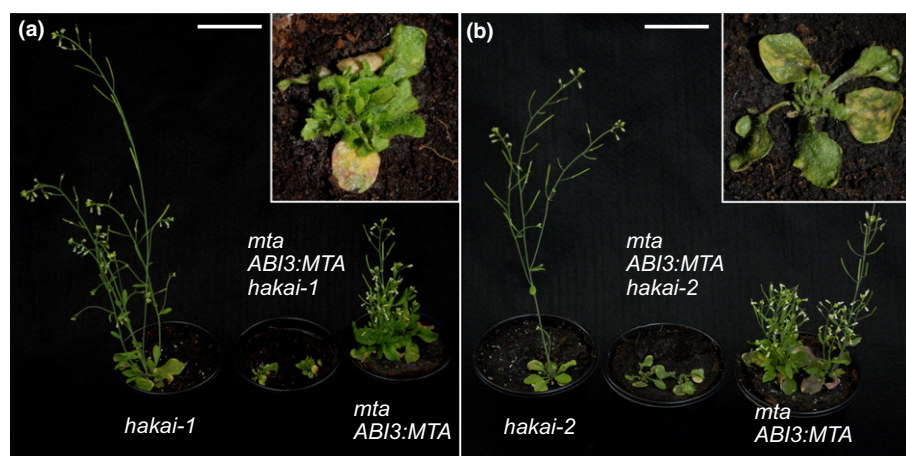


Fig. 8 *Arabidopsis thaliana* plants homozygous for either (a) *hakai-1* or (b) *hakai-2* crossed with *mta* *ABI3prom:MTA* show more severe developmental defects than either parent on its own (double mutants magnified in inset). Bars, 5 cm.

the conserved role of VIRILIZER, although whether this large protein is performing a scaffolding role or is catalytically active (and/or carries out a regulatory function) remains to be tested.

HAKAI is a new element required for the function of the *Arabidopsis* m⁶A writer complex and directly interacts with its core components

Mammalian HAKAI, also known as Casitas B-lineage lymphoma-transforming sequence-like protein 1 (CBLL1), was

initially identified as an E3 ubiquitin ligase that facilitates endocytosis of E-cadherin at cell–cell contacts, thus regulating epithelial integrity (Fujita *et al.*, 2002). More recently, it has also been implicated with influencing RNA–protein interactions in animal systems (Fujita *et al.*, 2002; Figueroa *et al.*, 2009) and has been reported in association with m⁶A writers (Horiuchi *et al.*, 2013), but a role in m⁶A writing has not been proposed until now. Although believed to act on E-cadherin complex at the plasma membrane, human and *D. melanogaster* HAKAIs are localized predominantly in the nucleus and in lower amounts at the plasma

membrane and in the cytoplasm (Figueroa *et al.*, 2009; Kaido *et al.*, 2009). *Arabidopsis* HAKAI-mCherry resides mainly in the nucleus (Fig. 3g). Plants lack cadherins and the mechanisms determining cell polarity are generally different in metazoans and plants (Kania *et al.*, 2014). Thus, the RNA-associated m⁶A-forming function of HAKAI that we identify here is likely to prevail in *Arabidopsis*. As phenotypes of *hakai* knockouts are rather subtle compared to the embryo lethality of other complex member knockouts, it is possible that HAKAI may have a more complex role. However, the extreme severity of the *hakai mta ABI3prom:MTA* and the lethality of the *hakai fip37-4* double mutants supports the conclusion that HAKAI is a *bona fide* functional member of the methylation complex. It also suggests that as methylation amounts drop below ~10% of wild-type (WT), the severity of growth phenotypes increases dramatically. The *mta ABI3prom:MTA* line was generated by complementing an *MTA* insertion knockout with an *MTA* coding sequence under control of the *ABI3* promoter, which drives high expression, and full m⁶A methylation, in seeds, but has very low activity post-germination (Bodi *et al.*, 2012). Thus, the combination of this genotype with *hakai* knockout would only be expected to show a double mutant phenotype post-germination. By contrast, the *fip37-4* hypomorph shows low levels of *FIP37* expression and has poor seed set even before combining with other mutant genotypes. Thus, selfing a plant that is homozygous for *fip37-4* and heterozygous for *hakai-2* would be expected to give a further, possibly developmentally lethal, reduction in m⁶A levels in the early stages of embryonic development.

HAKAI has been extensively studied in mammals due to its connection with oncogenesis (Aparicio *et al.*, 2012), primarily attributed to its controlling of cell–cell adhesion (Fujita *et al.*, 2002). However, it has been reported that this protein, through an uncharacterized mechanism, interacts with polypyrimidine tract binding protein associated splicing factor (PSF) and promotes its ability to bind specific (particularly tumorigenesis related) transcripts (Figueroa *et al.*, 2009). Mammalian HAKAI specifically ubiquitinates phosphotyrosine modified E-cadherin (Fujita *et al.*, 2002) and it may be that a similar mechanism is required for its activity within the m⁶A writer complex. Given the association of this protein with the writer complex in both plants and animals, and considering that in plants it is required for normal m⁶A methylation amounts, we propose that HAKAI is likely to also play a similar role in mRNA methylation in mammals. In this context, our findings could improve understanding of the mechanistic role of HAKAI in promoting tumorigenesis and regulating the binding of PSF with cancer-associated mRNA transcripts.

Acknowledgements

Supported by the Czech Science Foundation (P501/12/0934), European Social Fund (CZ.1.07/2.3.00/20.0189), the Ministry of Education, Youth and Sports of the Czech Republic (the National Program for Sustainability, NPU1-LQ1601 the NCLG Research Infrastructure, LM2015091, and the Czech-Biomaging, LM2015062) to K.R., M.S. and J.H. RNA methylation work in

R.G.F.'s lab was supported by the Biotechnology and Biological Sciences Research Council (grant nos. BB/K013637/1 and BB/M008606/1). Y.H.'s laboratory was funded by the Gatsby Foundation (GAT3395/PR3); the National Science Foundation Biotechnology and Biological Sciences Research Council grant (BB/N013158/1); University of Helsinki (award 799992091), the European Research Council Advanced Investigator Grant SYMDEV (no. 323052); the Finnish Funding Agency for Technology and Innovation (Tekes); and the Academy of Finland Centre of Excellence program (award 63053034). We thank G. G. Simpson for help with first versions of the manuscript and comments, A.-P. Mähönen and D. Reňák for sharing published materials, M. Frilander and J. Mravec for discussions, and P. Némec for technical assistance.

Author contributions

K.R., M.Z., A.C., Z.B., M.K., M.S., H.L. and S.Z. conducted experiments; A.C. performed genetic screen; D.E. and G.D.J. made the TAP experiment; S.E.-S. and N.P.M. carried out bioinformatics analyses; K.R., J.H., R.G.F. and Y.H. conceived research and designed experiments; and K.R. and R.G.F. wrote the manuscript. All authors read and commented on the final version of the manuscript.

References

- Agarwala SD, Blitzblau HG, Hochwagen A, Fink GR. 2012. RNA methylation by the MIS complex regulates a cell fate decision in yeast. *PLoS Genetics* 8: e1002732.
- Alarcón CR, Goodarzi H, Lee H, Liu X, Tavazoie S, Tavazoie SF. 2015a. HNRNPA2B1 is a mediator of m⁶A-dependent nuclear RNA processing events. *Cell* 162: 1299–1308.
- Alarcón CR, Lee H, Goodarzi H, Halberg N, Tavazoie SF. 2015b. N⁶-methyladenosine marks primary microRNAs for processing. *Nature* 519: 482–485.
- Anders S, Huber W. 2010. Differential expression analysis for sequence count data. *Genome Biology* 11: R106.
- Aparicio LA, Valladares M, Blanco M, Alonso G, Figueroa A. 2012. Biological influence of Haki in cancer: a 10-year review. *Cancer Metastasis Reviews* 31: 375–386.
- Bishopp A, Help H, El-Showk S, Weijers D, Scheres B, Friml J, Benková E, Mähönen AP, Helariutta Y. 2011. A mutually inhibitory interaction between auxin and cytokinin specifies vascular pattern in roots. *Current Biology* 21: 917–926.
- Bodi Z, Bottley A, Archer N, May ST, Fray RG. 2015. Yeast m⁶A methylated mRNAs are enriched on translating ribosomes during meiosis, and under rapamycin treatment. *PLoS ONE* 10: e0132090.
- Bodi Z, Zhong S, Mehra S, Song J, Graham N, Li H, May S, Fray RG. 2012. Adenosine methylation in *Arabidopsis* mRNA is associated with the 3' end and reduced levels cause developmental defects. *Frontiers in Plant Science* 3: 48.
- Bokar JA, Rath-Shambaugh ME, Ludwiczak R, Narayan P, Rottman F. 1994. Characterization and partial purification of mRNA N⁶-adenosine methyltransferase from HeLa cell nuclei. Internal mRNA methylation requires a multisubunit complex. *Journal of Biological Chemistry* 269: 17 697–17 704.
- Bokar JA, Shambaugh ME, Polayes D, Matera AG, Rottman FM. 1997. Purification and cDNA cloning of the AdoMet-binding subunit of the human mRNA (N⁶-adenosine)-methyltransferase. *RNA (New York, N.Y.)* 3: 1233–1247.
- Bujnicki JM, Feder M, Radlinska M, Blumenthal RM. 2002. Structure prediction and phylogenetic analysis of a functionally diverse family of proteins

- homologous to the MT-A70 subunit of the human mRNA: m⁶A methyltransferase. *Journal of Molecular Evolution* 55: 431–444.
- Caño-Delgado A, Lee J-Y, Demura T. 2010. Regulatory mechanisms for specification and patterning of plant vascular tissues. *Annual Review of Cell and Developmental Biology* 26: 605–637.
- Clancy MJ, Shambaugh ME, Timpert CS, Bokar JA. 2002. Induction of sporulation in *Saccharomyces cerevisiae* leads to the formation of N⁶-methyladenosine in mRNA: a potential mechanism for the activity of the IME4 gene. *Nucleic Acids Research* 30: 4509–4518.
- Dobin A, Davis CA, Schlesinger F, Drenkow J, Zaleski C, Jha S, Batut P, Chaisson M, Gingeras TR. 2013. STAR: ultrafast universal RNA-seq aligner. *Bioinformatics* 29: 15–21.
- Dominissini D, Moshitch-Moshkovitz S, Schwartz S, Salmon-Divon M, Ungar L, Osenberg S, Cesarkas K, Jacob-Hirsch J, Amariglio N, Kupiec M *et al.* 2012. Topology of the human and mouse m⁶A RNA methylomes revealed by m⁶A-seq. *Nature* 485: 201–206.
- Du Z, Zhou X, Ling Y, Zhang Z, Su Z. 2010. agriGO: a GO analysis toolkit for the agricultural community. *Nucleic Acids Research* 38: W64–W70.
- Edgren H, Murumagi A, Kangaspeka S, Nicorici D, Hongisto V, Kleivi K, Rye IH, Nyberg S, Wolf M, Borresen-Dale A-L *et al.* 2011. Identification of fusion genes in breast cancer by paired-end RNA-sequencing. *Genome Biology* 12: R6.
- Fang Y, Hearn S, Spector DL. 2004. Tissue-specific expression and dynamic organization of SR splicing factors in *Arabidopsis*. *Molecular Biology of the Cell* 15: 2664–2673.
- Figueroa A, Kotani H, Toda Y, Mazan-Mamczarz K, Mueller E-C, Otto A, Disch L, Norman M, Ramdasi RM, Keshtgar M *et al.* 2009. Novel roles of Hakai in cell proliferation and oncogenesis. *Molecular Biology of the Cell* 20: 3533–3542.
- Fray RG, Simpson GG. 2015. The *Arabidopsis* epitranscriptome. *Current Opinion in Plant Biology* 27: 17–21.
- Friml J, Benková E, Blilou I, Wisniewska J, Hamann T, Ljung K, Woody S, Sandberg G, Scheres B, Jürgens G *et al.* 2002. AtPIN4 mediates sink-driven auxin gradients and root patterning in *Arabidopsis*. *Cell* 108: 661–673.
- Fujita Y, Krause G, Scheffner M, Zechner D, Leddy HEM, Behrens J, Sommer T, Birchmeier W. 2002. Hakai, a c-Cbl-like protein, ubiquitinates and induces endocytosis of the E-cadherin complex. *Nature Cell Biology* 4: 222–231.
- Furuta KM, Yadav SR, Lehesranta S, Belevich I, Miyashima S, Heo J, Vátén A, Lindgren O, De Rybel B, Van Isterdael G *et al.* 2014. Plant development. *Arabidopsis* NAC45/86 direct sieve element morphogenesis culminating in enucleation. *Science (New York, N.Y.)* 345: 933–937.
- Fustin J-M, Doi M, Yamaguchi Y, Hida H, Nishimura S, Yoshida M, Isagawa T, Morioka MS, Kakeya H, Manabe I *et al.* 2013. RNA-methylation-dependent RNA processing controls the speed of the circadian clock. *Cell* 155: 793–806.
- Geldner N, Dénervaud-Tendon V, Hyman DL, Mayer U, Stierhof Y-D, Chory J. 2009. Rapid, combinatorial analysis of membrane compartments in intact plants with a multicolor marker set. *Plant Journal* 59: 169–178.
- Geula S, Moshitch-Moshkovitz S, Dominissini D, Mansour AA, Kol N, Salmon-Divon M, Herschkovitz V, Peer E, Mor N, Manor YS *et al.* 2015. m⁶A mRNA methylation facilitates resolution of naïve pluripotency toward differentiation. *Science* 347: 1002–1006.
- Gleave AP. 1992. A versatile binary vector system with a T-DNA organisational structure conducive to efficient integration of cloned DNA into the plant genome. *Plant Molecular Biology* 20: 1203–1207.
- Grabov A, Ashley MK, Rigas S, Hatzopoulos P, Dolan L, Vicente-Agullo F. 2005. Morphometric analysis of root shape. *New Phytologist* 165: 641–651.
- Hausmann IU, Bodi Z, Sanchez-Moran E, Mongan NP, Archer N, Fray RG, Soller M. 2016. m⁶A potentiates Sxl alternative pre-mRNA splicing for robust *Drosophila* sex determination. *Nature* 540: 301–304.
- Hilfiker A, Amrein H, Dübendorfer A, Schneiter R, Nöthiger R. 1995. The gene *virilizer* is required for female-specific splicing controlled by *Sxl*, the master gene for sexual development in *Drosophila*. *Development (Cambridge, England)* 121: 4017–4026.
- Hongay CF, Orr-Weaver TL. 2011. *Drosophila* Inducer of MEiosis 4 (IME4) is required for Notch signaling during oogenesis. *Proceedings of the National Academy of Sciences, USA* 108: 14 855–14 860.
- Horiuchi K, Kawamura T, Iwanari H, Ohashi R, Naito M, Kodama T, Hamakubo T. 2013. Identification of Wilms' tumor 1-associating protein complex and its role in alternative splicing and the cell cycle. *Journal of Biological Chemistry* 288: 33 292–33 302.
- Horowitz S, Horowitz A, Nilsen TW, Munns TW, Rottman FM. 1984. Mapping of N⁶-methyladenosine residues in bovine prolactin mRNA. *Proceedings of the National Academy of Sciences, USA* 81: 5667–5671.
- Ito T, Chiba T, Ozawa R, Yoshida M, Hattori M, Sakaki Y. 2001. A comprehensive two-hybrid analysis to explore the yeast protein interactome. *Proceedings of the National Academy of Sciences, USA* 98: 4569–4574.
- Jia G, Fu Y, Zhao X, Dai Q, Zheng G, Yang Y, Yi C, Lindahl T, Pan T, Yang Y-G *et al.* 2011. N⁶-Methyladenosine in nuclear RNA is a major substrate of the obesity-associated FTO. *Nature Chemical Biology* 7: 885–887.
- Kaido M, Wada H, Shindo M, Hayashi S. 2009. Essential requirement for RING finger E3 ubiquitin ligase Hakai in early embryonic development of *Drosophila*. *Genes to Cells* 14: 1067–1077.
- Kania U, Fendrych M, Friml J. 2014. Polar delivery in plants; commonalities and differences to animal epithelial cells. *Open Biology* 4: 140017.
- Karimi M, Depicker A, Hilson P. 2007. Recombinational cloning with plant gateway vectors. *Plant Physiology* 145: 1144–1154.
- Ke S, Alemu EA, Mertens C, Gantman EC, Fak JJ, Mele A, Haripal B, Zucker-Scharff I, Moore MJ, Park CY *et al.* 2015. A majority of m⁶A residues are in the last exons, allowing the potential for 3' UTR regulation. *Genes & Development* 29: 2037–2053.
- Kleinboelting N, Huep G, Kloetgen A, Viehoveer P, Weissshaar B. 2012. GABI-Kat SimpleSearch: new features of the *Arabidopsis thaliana* T-DNA mutant database. *Nucleic Acids Research* 40: D1211–D1215.
- Koegl M, Uetz P. 2007. Improving yeast two-hybrid screening systems. *Briefings in Functional Genomics & Proteomics* 6: 302–312.
- Lahav R, Gammie A, Tavazoie S, Rose MD. 2007. Role of transcription factor Kar4 in regulating downstream events in the *Saccharomyces cerevisiae* pheromone response pathway. *Molecular and Cellular Biology* 27: 818–829.
- Lence T, Akhtar J, Bayer M, Schmid K, Spindler L, Ho CH, Kreim N, Andrade-Navarro MA, Poeck B, Helm M *et al.* 2016. m⁶A modulates neuronal functions and sex determination in *Drosophila*. *Nature* 540: 242–247.
- Letunic I, Doerks T, Bork P. 2012. SMART 7: recent updates to the protein domain annotation resource. *Nucleic Acids Research* 40: D302–D305.
- Li Y, Wang X, Li C, Hu S, Yu J, Song S. 2014. Transcriptome-wide N⁶-methyladenosine profiling of rice callus and leaf reveals the presence of tissue-specific competitors involved in selective mRNA modification. *RNA Biology* 11: 1180–1188.
- Liu N, Dai Q, Zheng G, He C, Parisien M, Pan T. 2015. N⁶-methyladenosine-dependent RNA structural switches regulate RNA-protein interactions. *Nature* 518: 560–564.
- Liu J, Yue Y, Han D, Wang X, Fu Y, Zhang L, Jia G, Yu M, Lu Z, Deng X *et al.* 2014. A METTL3-METTL14 complex mediates mammalian nuclear RNA N⁶-adenosine methylation. *Nature Chemical Biology* 10: 93–95.
- Lorković ZJ, Hilscher J, Barta A. 2008. Co-localisation studies of *Arabidopsis* SR splicing factors reveal different types of speckles in plant cell nuclei. *Experimental Cell Research* 314: 3175–3186.
- Luo G-Z, MacQueen A, Zheng G, Duan H, Dore LC, Lu Z, Liu J, Chen K, Jia G, Bergelson J *et al.* 2014. Unique features of the m⁶A methylome in *Arabidopsis thaliana*. *Nature Communications* 5: 5630.
- Machnicka MA, Milanowska K, Osman Oglou O, Purta E, Kurkowska M, Olchowik A, Januszewski W, Kalinowski S, Dunin-Horkawicz S, Rother KM *et al.* 2013. MODOMICS: a database of RNA modification pathways – 2013 update. *Nucleic Acids Research* 41: D262–D267.
- Mähönen AP, Bishopp A, Higuchi M, Nieminen KM, Kinoshita K, Törmäkangas K, Ikeda Y, Oka A, Kakimoto T, Helariutta Y. 2006. Cytokinin signaling and its inhibitor AHP6 regulate cell fate during vascular development. *Science (New York, N.Y.)* 311: 94–98.
- Mähönen AP, ten Tusscher K, Siligato R, Smetana O, Díaz-Triviño S, Salojärvi J, Wachsmann G, Prasad K, Heidstra R, Scheres B. 2014. PLETHORA gradient formation mechanism separates auxin responses. *Nature* 515: 125–129.
- Meyer KD, Jaffrey SR. 2014. The dynamic epitranscriptome: N⁶-methyladenosine and gene expression control. *Nature Reviews. Molecular Cell Biology* 15: 313–326.

- Meyer KD, Saletore Y, Zumbo P, Elemento O, Mason CE, Jaffrey SR. 2012. Comprehensive analysis of mRNA methylation reveals enrichment in 3' UTRs and near stop codons. *Cell* 149: 1635–1646.
- Narayan P, Rottman FM. 1988. An *in vitro* system for accurate methylation of internal adenosine residues in messenger RNA. *Science* 242: 1159–1162.
- Nekrasov V, Staskawicz B, Weigel D, Jones JDG, Kamoun S. 2013. Targeted mutagenesis in the model plant *Nicotiana benthamiana* using Cas9 RNA-guided endonuclease. *Nature Biotechnology* 31: 691–693.
- Niessen M, Schneiter R, Nothiger R. 2001. Molecular identification of *virilizer*, a gene required for the expression of the sex-determining gene *Sex-lethal* in *Drosophila melanogaster*. *Genetics* 157: 679–688.
- Ortega A, Niksic M, Bachi A, Wilm M, Sánchez L, Hastie N, Valcárcel J. 2003. Biochemical function of Female-lethal (2)D/Wilms' tumor suppressor-1-associated proteins in alternative pre-mRNA splicing. *Journal of Biological Chemistry* 278: 3040–3047.
- Pekárová B, Klumpler T, Trisková O, Horák J, Jansen S, Dopitová R, Borkovcová P, Papoušková V, Nejedlá E, Sklenář V *et al.* 2011. Structure and binding specificity of the receiver domain of sensor histidine kinase CKI1 from *Arabidopsis thaliana*. *Plant Journal* 67: 827–839.
- Ping X-L, Sun B-F, Wang L, Xiao W, Yang X, Wang W-J, Adhikari S, Shi Y, Lv Y, Chen Y-S *et al.* 2014. Mammalian WTAP is a regulatory subunit of the RNA N⁶-methyladenosine methyltransferase. *Cell Research* 24: 177–189.
- Punta M, Coghill PC, Eberhardt RY, Mistry J, Tate J, Boursnell C, Pang N, Forslund K, Ceric G, Clements J *et al.* 2012. The Pfam protein families database. *Nucleic Acids Research* 40: D290–D301.
- Reddy ASN, Day IS, Göhring J, Barta A. 2012. Localization and dynamics of nuclear speckles in plants. *Plant Physiology* 158: 67–77.
- Ruzicka K, Strader LC, Bailly A, Yang H, Blakeslee J, Langowski L, Nejedlá E, Fujita H, Itoh H, Syono K *et al.* 2010. *Arabidopsis* PIS1 encodes the ABCG37 transporter of auxinic compounds including the auxin precursor indole-3-butyric acid. *Proceedings of the National Academy of Sciences, USA* 107: 10749–10753.
- Schneeberger K, Ossowski S, Lanz C, Juul T, Petersen AH, Nielsen KL, Jørgensen J-E, Weigel D, Andersen SU. 2009. SHOREmap: simultaneous mapping and mutation identification by deep sequencing. *Nature Methods* 6: 550–551.
- Schneider CA, Rasband WS, Eliceiri KW. 2012. NIH Image to ImageJ: 25 years of image analysis. *Nature Methods* 9: 671–675.
- Schwartz S, Mumbach MR, Jovanovic M, Wang T, Maciag K, Bushkin GG, Mertins P, Ter-Ovanesyan D, Habib N, Cacchiarelli D *et al.* 2014. Perturbation of m⁶A writers reveals two distinct classes of mRNA methylation at internal and 5' sites. *Cell Reports* 8: 284–296.
- Shen L, Liang Z, Gu X, Chen Y, Teo ZWN, Hou X, Cai WM, Dedon PC, Liu L, Yu H. 2016. N⁶-methyladenosine RNA modification regulates shoot stem cell fate in *Arabidopsis*. *Developmental Cell* 38: 186–200.
- Shen S, Park JW, Lu Z, Lin L, Henry MD, Wu YN, Zhou Q, Xing Y. 2014. rMATS: robust and flexible detection of differential alternative splicing from replicate RNA-Seq data. *Proceedings of the National Academy of Sciences, USA* 111: E5593–E5601.
- Sievers F, Wilm A, Dineen D, Gibson TJ, Karplus K, Li W, Lopez R, McWilliam H, Remmert M, Söding J *et al.* 2011. Fast, scalable generation of high-quality protein multiple sequence alignments using Clustal Omega. *Molecular Systems Biology* 7: 539.
- Siligato R, Wang X, Yadav SR, Lehesranta S, Ma G, Ursache R, Sevillem I, Zhang J, Gorte M, Prasad K *et al.* 2016. MultiSite Gateway-compatible cell type-specific gene-inducible system for plants. *Plant Physiology* 170: 627–641.
- Spector DL, Lamond AI. 2011. Nuclear Speckles. *Cold Spring Harbor Perspectives in Biology* 3: a000646.
- Tillemans V, Leponce I, Rausin G, Dispa L, Motte P. 2006. Insights into nuclear organization in plants as revealed by the dynamic distribution of *Arabidopsis* SR splicing factors. *Plant Cell* 18: 3218–3234.
- Tzafirir I, Dickerman A, Brazhnik O, Nguyen Q, McElver J, Frye C, Patton D, Meinke D. 2003. The Arabidopsis SeedGenes Project. *Nucleic Acids Research* 31: 90–93.
- Tzafirir I, Pena-Muralla R, Dickerman A, Berg M, Rogers R, Hutchens S, Sweeney TC, McElver J, Aux G, Patton D *et al.* 2004. Identification of genes required for embryo development in *Arabidopsis*. *Plant Physiology* 135: 1206–1220.
- Van Leene J, Eeckhout D, Persiau G, Van De Slijke E, Geerinck J, Van Isterdael G, Witters E, De Jaeger G. 2011. Isolation of transcription factor complexes from *Arabidopsis* cell suspension cultures by tandem affinity purification. *Methods in Molecular Biology (Clifton, N.J.)* 754: 195–218.
- Van Leene J, Hollunder J, Eeckhout D, Persiau G, Van De Slijke E, Stals H, Van Isterdael G, Verkest A, Neirynck S, Buffel Y *et al.* 2010. Targeted interactomics reveals a complex core cell cycle machinery in *Arabidopsis thaliana*. *Molecular Systems Biology* 6: 397.
- Van Leene J, Stals H, Eeckhout D, Persiau G, Van De Slijke E, Van Isterdael G, De Clercq A, Bonnet E, Laukens K, Remmerie N *et al.* 2007. A tandem affinity purification-based technology platform to study the cell cycle interactome in *Arabidopsis thaliana*. *Molecular & Cellular Proteomics* 6: 1226–1238.
- Van Leene J, Witters E, Inzé D, De Jaeger G. 2008. Boosting tandem affinity purification of plant protein complexes. *Trends in Plant Science* 13: 517–520.
- Vespa L, Vachon G, Berger F, Perazza D, Faure J-D, Herzog M. 2004. The immunophilin-interacting protein AtFIP37 from *Arabidopsis* is essential for plant development and is involved in trichome endoreduplication. *Plant Physiology* 134: 1283–1292.
- Wan Y, Tang K, Zhang D, Xie S, Zhu X, Wang Z, Lang Z. 2015. Transcriptome-wide high-throughput deep m⁶A-seq reveals unique differential m⁶A methylation patterns between three organs in *Arabidopsis thaliana*. *Genome Biology* 16: 272.
- Wang X, Lu Z, Gomez A, Hon GC, Yue Y, Han D, Fu Y, Parisien M, Dai Q, Jia G *et al.* 2014a. N⁶-methyladenosine-dependent regulation of messenger RNA stability. *Nature* 505: 117–120.
- Wang X, Zhao BS, Roundtree IA, Lu Z, Han D, Ma H, Weng X, Chen K, Shi H, He C. 2015. N⁶-methyladenosine modulates messenger RNA translation efficiency. *Cell* 161: 1388–1399.
- Wang Y, Li Y, Toth JI, Petroski MD, Zhang Z, Zhao JC. 2014b. N⁶-methyladenosine modification destabilizes developmental regulators in embryonic stem cells. *Nature Cell Biology* 16: 191–198.
- Waterhouse AM, Procter JB, Martin DMA, Clamp M, Barton GJ. 2009. Jalview Version 2 – a multiple sequence alignment editor and analysis workbench. *Bioinformatics* 25: 1189–1191.
- Xiao W, Adhikari S, Dahal U, Chen Y-S, Hao Y-J, Sun B-F, Sun H-Y, Li A, Ping X-L, Lai W-Y *et al.* 2016. Nuclear m⁶A reader YTHDC1 regulates mRNA splicing. *Molecular Cell* 61: 507–519.
- Yue Y, Liu J, He C. 2015. RNA N⁶-methyladenosine methylation in post-transcriptional gene expression regulation. *Genes & Development* 29: 1343–1355.
- Zheng G, Dahl JA, Niu Y, Fedorcsak P, Huang C-M, Li CJ, Vågbo CB, Shi Y, Wang W-L, Song S-H *et al.* 2013. ALKBH5 is a mammalian RNA demethylase that impacts RNA metabolism and mouse fertility. *Molecular Cell* 49: 18–29.
- Zhong S, Li H, Bodi Z, Button J, Vespa L, Herzog M, Fray RG. 2008. MTA is an *Arabidopsis* messenger RNA adenosine methylase and interacts with a homolog of a sex-specific splicing factor. *Plant Cell* 20: 1278–1288.
- Zhou J, Wan J, Gao X, Zhang X, Jaffrey SR, Qian S-B. 2015. Dynamic m⁶A mRNA methylation directs translational control of heat shock response. *Nature* 526: 591–594.

Supporting Information

Additional Supporting Information may be found online in the Supporting Information tab for this article:

Fig. S1 Sequence conservation of VIR homologues.

Fig. S2 Additional molecular and phenotypic characterization of *vir-1*.

Fig. S3 Sequence conservation of HAKAI homologues.

Fig. S4 Expression of VIR and other proteins associated with m⁶A writing in the root tip.

Fig. S5 m⁶A levels are reduced in adult *hakai-2*, *mta ABI3prom:MTA* and their double mutant combination.

Table S1 Summary of oligonucleotides used in this study

Table S2 Summary of splicing events altered in the *vir-1* background

Table S3 List of genes with significantly changed expression in the *vir-1* root tips as determined by the DESEQ software package

Table S4 Summary of gene ontology (GO) analysis of genes mis-expressed in the *vir-1* mutants.

Table S5 Establishing list of genes required for vascular formation

Table S6 List of genes involved in vascular formation, which show altered expression in the *vir-1* root tips

Table S7 TAP-VIR proteomics data

Please note: Wiley Blackwell are not responsible for the content or functionality of any Supporting Information supplied by the authors. Any queries (other than missing material) should be directed to the *New Phytologist* Central Office.



About New Phytologist

- *New Phytologist* is an electronic (online-only) journal owned by the New Phytologist Trust, a **not-for-profit organization** dedicated to the promotion of plant science, facilitating projects from symposia to free access for our Tansley reviews.
- Regular papers, Letters, Research reviews, Rapid reports and both Modelling/Theory and Methods papers are encouraged. We are committed to rapid processing, from online submission through to publication 'as ready' via *Early View* – our average time to decision is <26 days. There are **no page or colour charges** and a PDF version will be provided for each article.
- The journal is available online at Wiley Online Library. Visit **www.newphytologist.com** to search the articles and register for table of contents email alerts.
- If you have any questions, do get in touch with Central Office (np-centraloffice@lancaster.ac.uk) or, if it is more convenient, our USA Office (np-usaoffice@lancaster.ac.uk)
- For submission instructions, subscription and all the latest information visit **www.newphytologist.com**